Engineering Fracture Mechanics Vol. 35, No. 1/2/3, pp. 219–231, 1990
Printed in Great Britain.

0013-7944/90 $3.00 + 0.00
Pergamon Press plc.

FINITE ELEMENT NONLINEAR ANALYSIS OF CONCRETE STRUCTURES USING A "PLASTIC-DAMAGE MODEL"

S. OLLER,† E. OÑATE,† J. OLIVER† and J. LUBLINER‡

†Universitat Politècnica de Catalunya, E.T.S. Ingenieros de Caminos, Canales y Puertos, Jordi Girona Salgado, 31-08034 Barcelona, Spain and

‡University of California, Department of Civil Engineering, Berkeley, CA 94720, U.S.A.

Abstract—In this paper a plastic damage model for nonlinear finite element analysis of concrete is presented. The model is based on standard plasticity theory for frictional materials. Details of the expressions of a new yield function proposed and of the evolution laws of the model parameters are given. The model allows to include elastic and plastic stiffness degradation effects. This is also discussed in the paper together with the problem of mesh objectivity, and the *a posteriori* determination of cracks. Finally, one example of application which shows the accuracy of the model is also given.

1. INTRODUCTION

IT IS WELL known that microcracking in concrete takes place at low load levels due to physical debonding between aggregate and mortar particles, or to simple microcracking in the mortar area. Cracking progresses following a non-homogeneous path which combines the two mentioned mechanisms with growth and linking between microcracks along different directions. Experiments carried out on mortar specimens show that the distribution of microcracking is fairly discontinuous with arbitrary orientations[1]. This fact is supported by many experiments which show that *cracking can be considered, at microscopic level, as a non-directional phenomenon* and that the propagation of microcracks at aggregate level follows an erratic path which depends on the size of the aggregate particles. Thus, *the dominant cracking directions can be interpreted at macroscopic level as the locus of trajectories of the damage points.*

The above concepts support *the idea that the nonlinear behaviour of concrete can be modelled using concepts of classical plasticity theory* provided an adequate yield function is defined for taking into account the different response of concrete under tension and compression states. Cracking can, therefore, be interpreted as a *local damage effect*, defined by the evolution of known material parameters and by a single yield function which controls the onset and evolution of damage.

One of the advantages of such a model is the independence of the analysis with respect to crack directions which can be simply identified *a posteriori* from the converged values of the nonlineal solution. This allows to overcome the problems associated to most elastic–brittle smeared cracking models such as the need for an uncoupled constitutive equation along each cracking direction[2–4], the use of an arbitrary defined shear retention factor[2, 4], the lack of equilibrium in the damage points when more than one crack is formed[2, 5], the difficulty of defining stress paths at the crack under complex loading/unloading conditions and the difficulty of combining cracking and plasticity phenomena at the damage points.

In this work an elastoplastic model for nonlinear analysis of concrete based on the concepts of *plastic damage* mentioned above is presented[6, 7]. The model takes into account all the important aspects which should be considered in the nonlinear analysis of concrete, such as the different response under tension and compression, the effect of stiffness degradation and the problem of objectivity of the results with respect to the finite element mesh.

The layout of the paper is as follows. First, details of the yield function and the evolution laws of all material parameters are given. Secondly, the effects of elastic and plastic stiffness degradations are briefly described. Then, the *problem of mesh objectivity* and the *a posteriori* determination of cracking is presented. Finally, an example of application showing the accuracy of the model for analysis of concrete structures is presented.

2. BASIC CONCEPTS OF THE "PLASTIC DAMAGE MODEL"

The proposed plastic damage model can be considered as a general form of classical plasticity in which the standard hardening variable is replaced by a normalized plastic damage variable κ^p, such that $0 \leq \kappa^p \leq 1$. This last variable is similar to the former in the sense that it never decreases and it only increases if plastic deformation takes place (which is associated to the existence of microcracking). The limit value of $\kappa^p = 1$ denotes total damage at a point with complete loss of cohesion. This can be interpreted as the formation of a macroscopic crack.

If stiffness degradation effects are neglected (and this will be separately treated in Section 8) the basic equations of the model are:

(a) *The yield function* defined as:

$$\mathscr{F}(\boldsymbol{\sigma}, \phi, c) = F(\boldsymbol{\sigma}, \phi) - c = 0, \tag{1}$$

where c is a cohesion or some constant multiple thereof, and ϕ is an internal friction angle. $F(\boldsymbol{\sigma}, \phi)$ is a function of the stress components that is first degree homogeneous in the stresses $\boldsymbol{\sigma}$, given a physical meaning of scaled stress to the cohesion. The particular forms of $\mathscr{F}$ used in this work are presented in Section 3.

(b) *The elasto-plastic strain decomposition* as:

$$\boldsymbol{\epsilon} = \mathbf{D}_S^{-1} \cdot \boldsymbol{\sigma} + \boldsymbol{\epsilon}^p = \boldsymbol{\epsilon}^e + \boldsymbol{\epsilon}^p \tag{2}$$

where $\mathbf{D}_S$ is the elastic constitutive matrix[6].

(c) *The flow rule* is defined for the general case of non-associated plasticity as:

$$\dot{\boldsymbol{\epsilon}}^p = \dot{\lambda} \frac{\partial \mathscr{G}(\boldsymbol{\sigma}, \psi\, c)}{\partial \boldsymbol{\sigma}} = \dot{\lambda} \mathbf{g} \tag{3}$$

where λ is the plastic loading factor, ψ is a dilatancy angle and $\mathbf{g}$ is a plastic flow vector, normal to the plastic potential surface $\mathscr{G}(\boldsymbol{\sigma}, \psi, c)$. From eqs (1)–(3) the standard elastoplastic incremental constitutive equation can be obtained as:

$$\dot{\boldsymbol{\sigma}} = \mathbf{D}^{ep} \cdot \dot{\boldsymbol{\epsilon}} \tag{4}$$

with the elastoplastic constitutive matrix given by:

$$\mathbf{D}_T^{ep} = \mathbf{D}_S - \frac{\left[\mathbf{D}_S \cdot \left\{\frac{\partial \mathscr{G}}{\partial \boldsymbol{\sigma}}\right\}\right] \otimes \left[\mathbf{D}_S \cdot \left\{\frac{\partial \mathscr{F}}{\partial \boldsymbol{\sigma}}\right\}\right]}{A + \left[\left\{\frac{\partial \mathscr{F}}{\partial \boldsymbol{\sigma}}\right\} \cdot \mathbf{D}_S \cdot \left\{\frac{\partial \mathscr{G}}{\partial \boldsymbol{\sigma}}\right\}\right]} \tag{5}$$

where A is the hardening parameter[6, 8]. Note from eq. (5) that $\mathbf{D}_T^{ep}$ is only symmetric for $\mathscr{G} = \mathscr{F}$ (associated plasticity).

(d) *The evolution laws for internal variables* κ^p and c of the form:

$$\dot{\kappa}^p = \dot{\lambda} \left[\mathbf{h}_\kappa(\boldsymbol{\sigma}, \kappa^p, c) \cdot \frac{\partial \mathscr{G}(\boldsymbol{\sigma}, \psi, c)}{\partial \boldsymbol{\sigma}} \right] = \mathbf{h}_\kappa(\boldsymbol{\sigma}, \kappa^p, c) \cdot \dot{\boldsymbol{\epsilon}}^p \tag{6}$$

$$\dot{c} = \dot{\lambda} \left[h_c(\boldsymbol{\sigma}, \kappa^p, c) \mathbf{h}_\kappa(\boldsymbol{\sigma}, \kappa^p, c) \cdot \frac{\partial \mathscr{G}(\boldsymbol{\sigma}, c)}{\partial \boldsymbol{\sigma}} \right] = h_c(\boldsymbol{\sigma}, \kappa^p, c)\, \kappa^{*p}. \tag{7}$$

The forms of functions $\mathbf{h}_\kappa$ and h_c will be given in Section 4 and 5, respectively. The cohesion c is a scaled uniaxial stress, so that its initial value c_0 coincides with the initial yield stress f_{c0} obtained from a uniaxial compression test. This value can be interpreted as a discontinuity stress, i.e. the stress for which the volumetric strain reaches a minimum. Therefore, $c = c_0 = f_{c0}$ for $\kappa^p = 0$, and $c = c_u = 0$ for $\kappa^p = 1$. Note, however, that c is not determined by an explicit function of κ^p, as is the case in simple plasticity models with isotropic hardening, but is itself an *internal variable*, depending on the load process, whose evolution is expressed by eq. (7).

3. DEFINITION OF THE YIELD SURFACE

Recent work[6, 9, 10, 11] has shown that the behaviour of concrete under triaxial compression states can be adequately modelled by yield criteria of the type of eq. (1) with $\mathscr{F}$ being a function with straight meridians, that is first degree homogeneous in the stress components.

In this work two different yield functions that satisfy the above requirement have been developed. The first one, used in the early stages of this work[12–14] is based on a simple modification of the well known Mohr–Coulomb yield surface as shown in Fig. 1. The new yield surface is monitored by a reduction parameter α_R which allows to shift the R–ϕ curve (R being the ratio between the maximum tension and compression stresses) towards a region in which the related values of R and ϕ are compatible with those of concrete ($\phi \simeq 30°$ for $R \simeq 10$)[13]. Numerical results obtained with this simple yield function were good and they can be seen in [12–14].

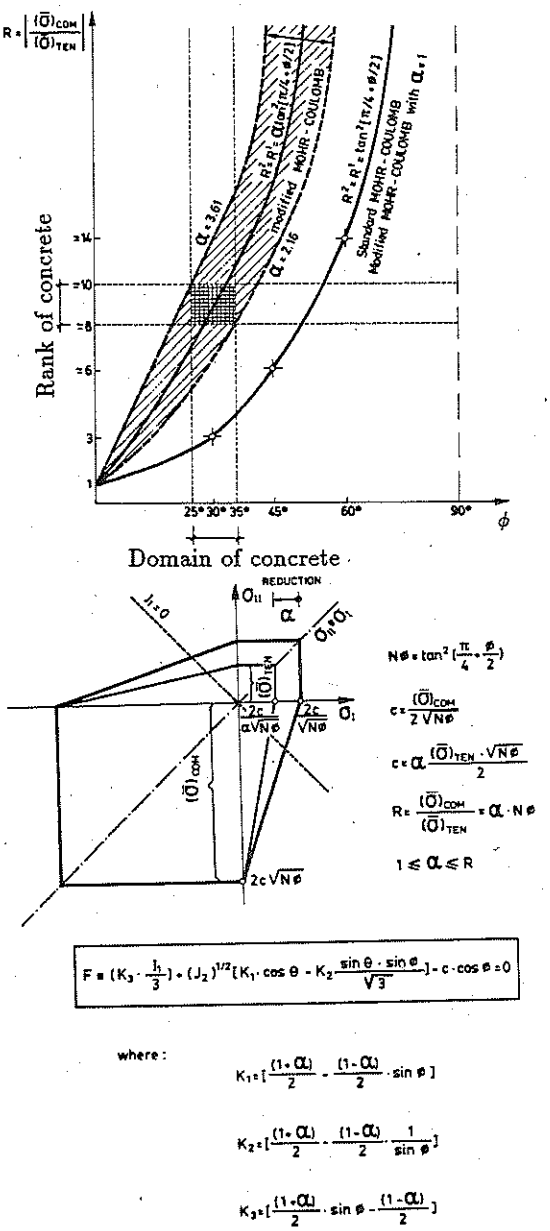

Fig. 1. R–ϕ ratios for Mohr–Coulomb and modified Mohr–Coulomb surface.

A more detailed study of the experimental work reported for biaxial and triaxial behaviour of concrete allowed the authors to define a new function of the form [6, 7] (Fig. 2).

$$\mathcal{F} = \mathcal{F}(\sigma, \phi, c) = \frac{1}{(1-\alpha)}[\sqrt{3J_2} + \alpha I_1 + \beta\langle\sigma^{\max}\rangle - \gamma\langle -\sigma^{\max}\rangle] - c = 0 \tag{8}$$

where I_1 is the first invariant of stress, α, β and γ are dimensionless parameters that can be expressed as functions of the friction angle ϕ, $\sigma^{\max}$ is the maximum principal stress and $\langle \pm x\rangle = \frac{1}{2}[x \pm |x|]$ is a ramp function. Note that when $\sigma^{\max} = 0$ (biaxial compression), $\mathcal{F}$ is just the Drucker–Prager criterion, with the exception of parameter α. This can be obtained comparing the initial equibiaxial compression stress f_{b0} with initial uniaxial compression stress f_{c0}, yielding[6, 7, 15]:

$$\alpha = \left(\frac{f_{b0}}{f_{c0}} - 1\right) \Big/ \left(2\frac{f_{b0}}{f_{c0}} - 1\right). \tag{9}$$

Experimental values give $1.10 \leq f_{b0}/f_{c0} \leq 1.16$ which yields $0.08 \leq \alpha \leq 0.1212\ldots$.

Once α is known, β can be determined from the value of $R = f_{c0}/f_{T0}$, where f_{T0} is the initial uniaxial tensile yield stress, as[6, 7, 15]:

$$\beta = (1-\alpha)R - (1+\alpha), \tag{10}$$

and for $R \simeq 10$ and $\alpha \simeq 0.10$ gives $\beta \simeq 7.50$.

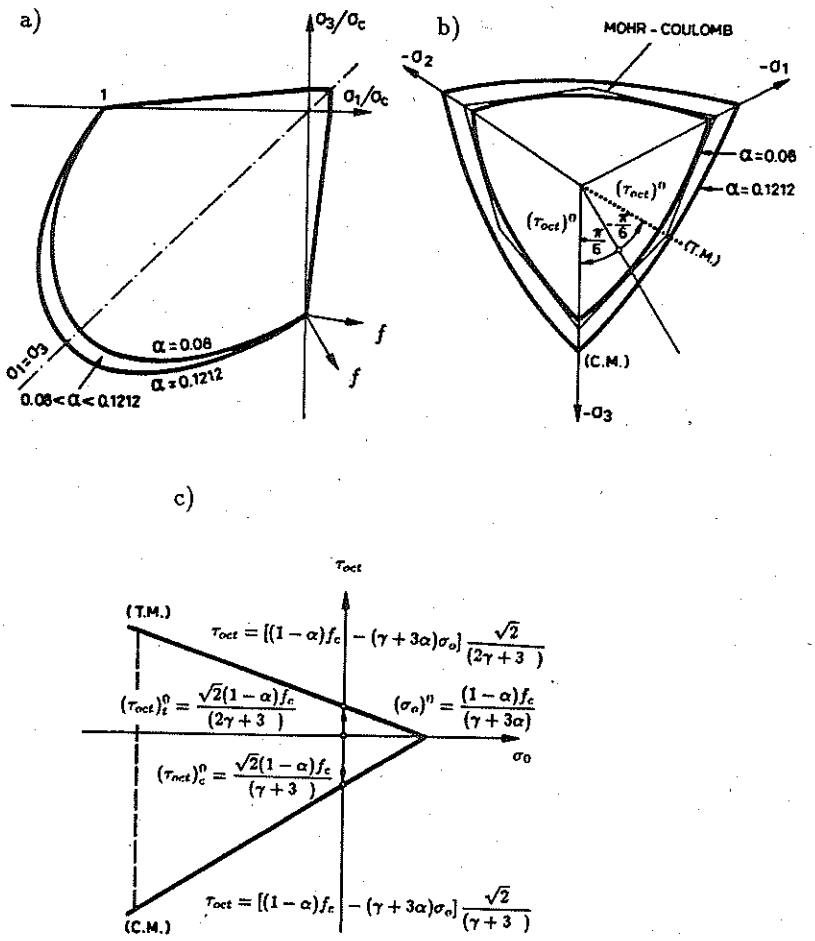

Fig. 2. Proposed yield surface: (a) (σ_{11}–σ_{33}; $\sigma_{22} = 0$) plane; (b) octahedral plane; (c) meridian plane.

The parameter γ appears only in triaxial compression with $\sigma^{max} < 0$. Considering the equations of the straight tension (TM) and compression (CM) meridians of the yield surface it can be obtained[6, 7]:

$$\gamma = \frac{3(1 - r_{oct}^{max})}{2r_{oct}^{max} - 1} \tag{11}$$

where:

$$r_{oct}^{max} = (\sqrt{J_2})_{TM}/(\sqrt{J_2})_{CM} \quad \text{at a given } I_1. \tag{12}$$

Experimental tests show that r_{oct}^{max} has a constant mean value of $\simeq 0.65$[6, 7] which yields a value of $\lambda \simeq 3.5$.

4. DEFINITION OF THE PLASTIC DAMAGE VARIABLE κ^p

Let us consider stress–plastic strain diagrams for uniaxial tension and compression tests (see Fig. 3). For each test we define:

$$\kappa^p = \frac{1}{g_T^p}\int_{t=0}^{t} \sigma_T \dot{\epsilon}_R^p \, dt, \quad \text{for uniaxial tension, and}$$

$$\kappa^p = \frac{1}{g_C^p}\int_{t=0}^{t} \sigma_C \dot{\epsilon}_C^p \, dt, \quad \text{for uniaxial compression} \tag{13}$$

where g_T^p and g_C^p are the specific plastic works, defined by the areas under each of the curves σ_T–ϵ_T^p and σ_C–ϵ_C^p (Fig. 3) obtained from the tension and compression uniaxial tests, respectively. The eqs (13) allow the transformation of uniaxial diagrams: $\sigma = f(\epsilon^p)$ in other: $\sigma = f(\kappa^p)$ such that (Fig. 4):

tension test: $f_T(0) = f_{T0}$ and $f_T(1) = 0$;

compression test: $f_C(0) = f_{C0}$ and $f_C(1) = 0$.

Starting from these concepts, the evolution law for κ^p can be generalized for a multiaxial stress state (written in terms of principal stress and plastic strain), as[6, 7, 16]:

$$\dot{\kappa}^p = \mathbf{h}_\kappa(\boldsymbol{\sigma}, \kappa^p, c) \cdot \dot{\boldsymbol{\epsilon}}^p = \sum_{i=1}^{3} (h_{\kappa i} \dot{\epsilon}_i^p) \tag{14}$$

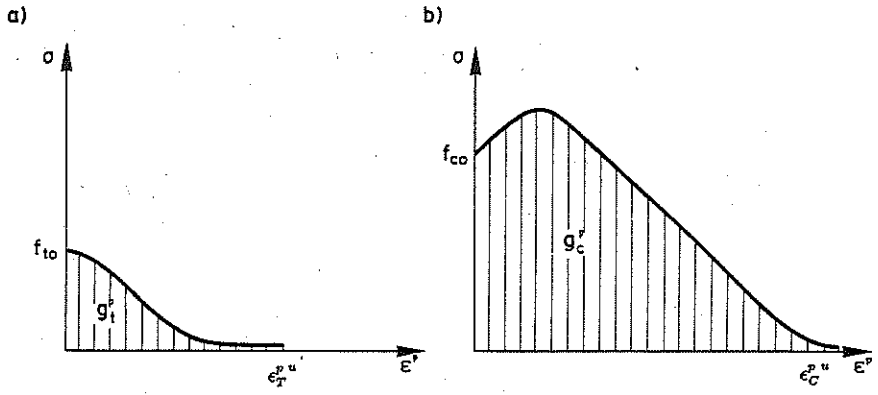

Fig. 3. Uniaxial curves (σ–ϵ^p). (a) Tension; (b) compression.

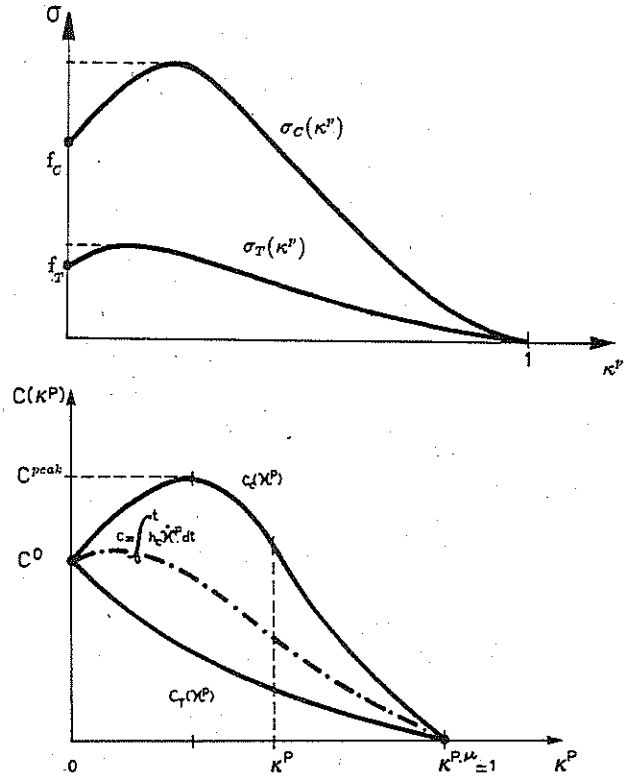

Fig. 4. Uniaxial curves: (1) tension and (2) compression. (a) Uniaxial curves ($\sigma-\kappa$), (b) uniaxial curves ($c-\kappa$).

with:

$$h_{\kappa i} = [(h_{\kappa i})_T + (h_{\kappa i})_C] = \frac{1}{g_T^{p*}} \langle \sigma_i \rangle + \frac{1}{g_C^{p*}} \langle -\sigma_i \rangle$$

$$g_T^{p*} = g_T^p \frac{\sum_{i=1}^{3} \langle \sigma_i \rangle}{\sigma_T}; \quad g_C^{p*} = g_C^p \frac{\sum_{i=1}^{3} \langle -\sigma_i \rangle}{\sigma_C} \tag{15}$$

where indices T and C denote values obtained from uniaxial tension and compression tests, respectively. In eq. (15) g_T^{p*} and g_C^{p*} are normalized values of the uniaxial specific plastic work for tension and compression processes, accordingly to the yield function chosen and also to the uniaxial tension and compression stresses σ_T and σ_C. For further details see [6, 7, 15, 16].

5. EVOLUTION LAW FOR THE INTERNAL VARIABLE OF COHESION c

The evolution of the cohesion c must satisfy $c \to 0$ for $\kappa^p \to 1$. In this model the evolution law for the cohesion is given by eq. (7) with the evolution function $h_c(\boldsymbol{\sigma}, \kappa^p, c)$ defined by[6, 7, 12, 15, 16]:

$$h_c(\boldsymbol{\sigma}, \kappa^p, c) = \left[\frac{r(\boldsymbol{\sigma})}{c_T(\kappa^p)} \frac{dc_T(\kappa^p)}{d\kappa^p} + \frac{1 - r(\boldsymbol{\sigma})}{c_C(\kappa^p)} \frac{dc_C(\kappa^p)}{d\kappa^p} \right] \tag{16}$$

where c is the actual value of the cohesion, $c_T(\kappa^p)$ and $c_C(\kappa^p)$ are the cohesion functions obtained from tension and compression uniaxial tests, respectively (see Fig. 4), and $r(\boldsymbol{\sigma})$ is a function defining

the stress stated, being $0 \leqslant r(\sigma) \leq 1$ with $r(\sigma) = 1$ if $\sigma_i \geq 0$ over all $i = 1, 2, 3$, and $r(\sigma) = 0$ if $\sigma_i \leq 0$ over all $i = 1, 2, 3$. We have taken:

$$r(\sigma) = \frac{\sum_{i=1}^{3} \langle \sigma_i \rangle}{\sum_{i=1}^{3} |\sigma_i|} \tag{17}$$

For further details the reader is referred to [6, 7, 15, 16].

6. EVOLUTION LAW FOR THE INTERNAL FRICTION ANGLE ϕ

It has been shown[6, 15, 17] that the loss of cohesion in concrete due to increase plastic damage affects the value of angle of internal friction, which ranges from $\phi \simeq 0$ for initial cohesion c_0 until $\phi = \phi^{\max}$ for the ultimate value of cohesion $c = c_u = 0$. In this work the following evolution law for ϕ has been chosen:

$$\sin \phi = \begin{cases} 2\dfrac{\sqrt{\kappa^p \kappa^L}}{\kappa^p + \kappa^L} \sin \phi^{\max}; & \forall\, \kappa^p \leq \kappa^L \\ \sin \phi^{\max}; & \forall\, \kappa^p > \kappa^L \end{cases} \tag{18}$$

where κ^L denotes the limit damage for which the value of ϕ remains constant (see Fig. 5).

7. PLASTIC POTENTIAL FUNCTION AND DILATANCY ANGLE ψ

Granular materials like concrete exhibit dilatancy phenomenon[6, 15, 17]. This can be modelled introducing an adequate plastic potential function $\mathcal{G}$ to match the numerical values obtained for the inelastic volume change with experimental data. In this work we have chosen for $\mathcal{G}$ the modified Mohr–Coulomb yield function (see Section 3) with the angle of dilatancy ψ substituting the internal friction angle ϕ. The evolution law for ψ has been obtained via a simple modificaton of the general expression proposed by Rowe for rocks and used by Vermeer and De Borst[17] for concrete as:

$$\psi(\kappa^p) = \arcsin\left[\frac{\sin \phi(\kappa^p) - \sin \phi_{cv}}{1 - \sin \phi(\kappa^p) \sin \phi_{cv}}\right] \tag{19}$$

where ϕ_{cv} can be taken as a constant value. For concrete $\phi_{cv} \simeq 13°$.

The eq. (19) gives for the initial stages of the process a negative dilatancy, which increases as plastic damage increases, takes a zero value for $\phi = \phi_{cv}$ and reaches a maximum for $\phi = \phi^{\max}$. For concrete a negative value of ψ has not physical meaning and, therefore, it must be taken $\phi = 0$ for $\phi \leq \phi_{cv}$ (see Fig. 6).

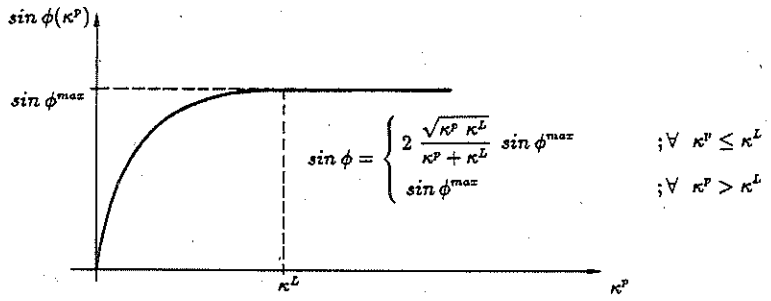

Fig. 5. Evolution law for the internal friction angle[17].

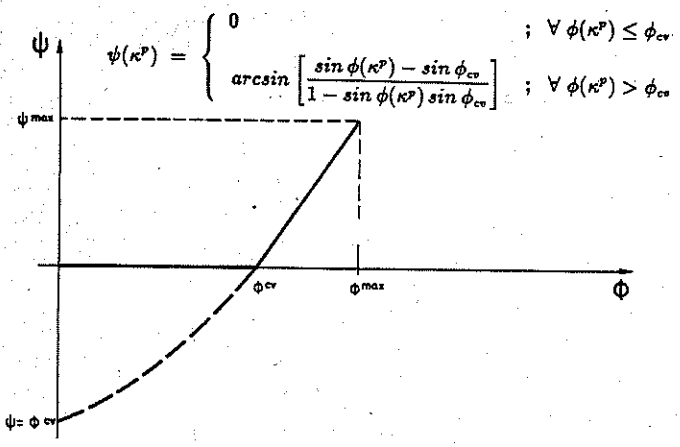

Fig. 6. Evolution law for the dilatancy angle[17].

8. GENERALIZATION OF THE MODEL TO INCLUDE STIFFNESS DEGRADATION

Experimental results show that near and beyond peak strength cemented granular materials exhibit an increasing degradation of stiffness due to microcracking (Fig. 7). The consideration of the phenomenon of stiffness degradation makes it necessary some modifications in the basic concepts of the theory of plasticity used in previous sections and, in particular, that of associated plasticity[6, 7].

Taking into account the stiffness degradation effects implies modifying the elastic secant constitutive matrix $\mathbf{D}_S$ in terms of two sets of internal variables: the elastic degradation variables and the plastic degradation variables whose evolutions will be assumed to be governed by rate equations of the form: $\dot{d}_i^e = \Phi_i \langle \mathbf{k}_i \cdot \dot{\epsilon} \rangle$ and $\dot{d}_j^p = \mathbf{l}_j \cdot \dot{\epsilon}^p$[6, 7, 18] respectively; where $\mathbf{k}_i$ and $\mathbf{l}_j$ are vectors in the stresses space denoting the directions of elastic and plastic degradation, respectively; and Φ_i is a positive scalar factor (for further details the reader is referred to [6, 7, 18].

In this paper we have used the simplest assumption for elastic degradation based on a simple isotropic degradation variable: d^e, such that the secant constitutive matrix is modified by:

$$\mathbf{D}_S(d^e) = (1 - d^e)\mathbf{D}^0 \tag{20}$$

where $\mathbf{D}^0$ is the initial stiffness. Parameter d^e can be interpreted as the ratio between the area of degradated material and the total area, and it can be expressed[6, 7]

$$d^e = 1 - e^{-\phi_{we,0}} \tag{21}$$

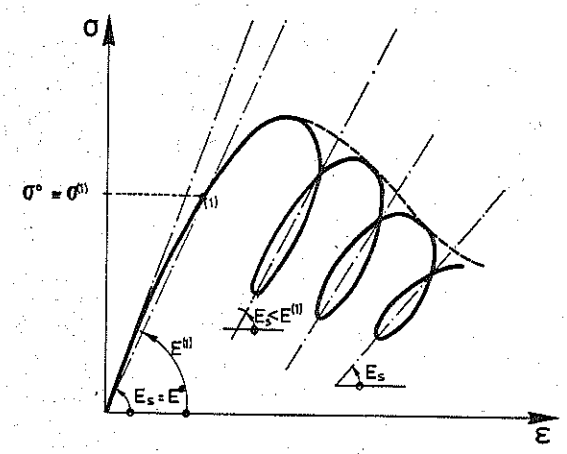

Fig. 7. Degradation of stiffness module due to microcracking.

where $2\,w^{e,0} = \epsilon^e \cdot \mathbf{D}^0 \cdot \epsilon^e$ is the square of the undamaged energy norm of the strain[19], ϵ^e is the elastic strain and Φ is a constant given for this particular case, by[6]:

$$\Phi = \frac{2}{E^0 (\epsilon^{e1})^2} \ln \frac{E^1}{E^0} \tag{22}$$

where E^0 is initial Young modulus; E^1 and ϵ^{e1} are the secant Young modulus and elastic deformation at the limit stress point of elastic degradation, respectively[6]. For further details the reader is referred to [6, 7].

For the plastic degradation a simple one-parameter model has also been used in this paper. This is based on the assumption that plastic degradation takes place only in the softening branch and that the stiffness is then proportional to the cohesion. The secant constitutive matrix is thus given by:

$$\mathbf{D}_S(d^p, \mathbf{d}^e) = (1 - d^p)\,\mathbf{D}_S(\mathbf{d}^e) \tag{23}$$

with the plastic degradation parameter d^p given by:

$$d^p = 1 - \frac{c}{c^{peak}} \tag{24}$$

where c is the actual value of cohesion and c^{peak} is the maximum cohesion value reached. For further details the reader is referred to [6, 7, 18].

9. PROBLEM OF OBJECTIVITY RESPONSE

See Ref. [7]. It has been made abundantly clear over the past decade that the strain-softening branch of the stress–strain curves cannot represent a local physical property of the material. The argument have been advanced both on physical grounds and on the basis of the mesh-sensitivity of numerical solutions obtained by means of the finite-element method. The mesh-sensitivity can be largely eliminated if one defines $g_T^p = G_T/l$ and $g_C^p = G_C/l$, where l is a charactristic length related to the mesh size, and G_T and G_C are quantities with the dimensions of energy/area that are assumed to be material properties.

In problems involving tensile cracking, G_T may be identified with the specific fracture energy G_f, defined as the energy required for form a unit area of crack. It has generally been assumed that G_f is a true material property, and methods have been developed for determining it[4]. For the characteristic length l, various approaches have been proposed[3, 20, 21].

Not so much attention has been paid to the corresponding compressive problem. Compressive failure may occur through several mechanisms—crushing, shearing and transverse cracking—and consequently G_c, if indeed it is a material property, cannot be readily identified with any particular physical energy. Moreover, it must be kept in mind that it is only the descending portion of the stress–strain curve that is mesh-sensitive.

10. NUMERICAL EXPERIMENTATION

The constitutive model presented has been implemented in a standard finite element program for nonlinear analysis of structures and applied to evaluate the numerical response of several specimens for which experimental results are known. Before entering in the discussion of the example analysed, some general considerations on the definition and representation of cracking have to be done.

Cracking is the most important external manifestation of damage in a concrete structure. In order to obtain a graphic representation of this kind of damage, some parameters are

evaluated, at each integration point *a posteriori*, once convergence of the nonlinear solution has been reached. This can be interpreted as a postprocessing of the results in which, conditions for onset of cracking, crack directions, plastic strains (as a measure at the opening of the cracks), energy dissipation and the shear retention factor are computed[6]. Cracking initiates at a point when the plastic-damage variable κ^p is greater than zero, and the maximum principal plastic strain is positive. Direction of cracking is assumed to be orthogonal to that of the maximum principal plastic strain at the damaged point. Other criteria for defining onset and directions of cracking the localization condition based on the acoustic tensor[22] or maximum energy release[1] are also possible.

Example: Prestressed cantilever beam

The beam shown in Fig. 8 has been subjected to a numerical test consisting of (a) prestressing in a direction parallel to the neutral axis, and (b) subsequent transversal loading as shown in Fig. 8. This corresponds to an experimental numerical test studied with some modifications by Rots *et al.* in [4]. The numerical data for this example has been obtained from [4].

The material parameter and finite element mesh used are shown in Fig. 8. Four node elements have been employed in the narrow band shown in Fig. 8, whereas eight node elements are used in the rest of the beam. 2×2 Gaussian quadrature has been used for all elements.

The load–displacement curve obtained is plotted in Fig. 9(a) Comparison of the obtained results with those presented in [4] is good. It can be seen that the applied load does not reach a zero value. This is due to the vertical component of the prestressing load, which opposes the opening of the two beam edges (see Fig. 9d). The dissipated energy is shown in Fig. 9(b) where it can be seen that the solution destabilizes to the correct value. In Fig. 9(c) the stress changes in the point under more severe damage is presented. Finally, Fig. 9(d) clearly shows the localization of deformation, crack and stress evolution. Again it is worth noting that the cracked elements simulate the effect of a single crack occurring in practice. Also note in Fig. 9(d) the small transverse cracks due to local bending of the two beam edges.

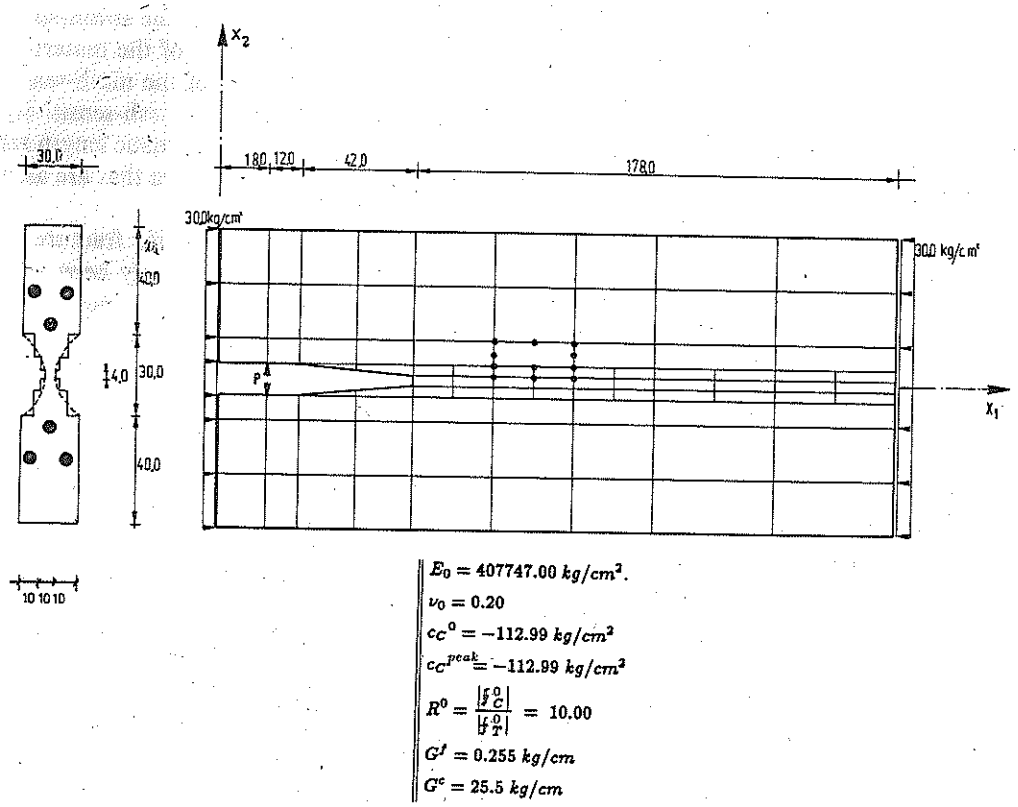

Fig. 8. *Prestressed beam.* Relevant material parameters, and finite element mesh.

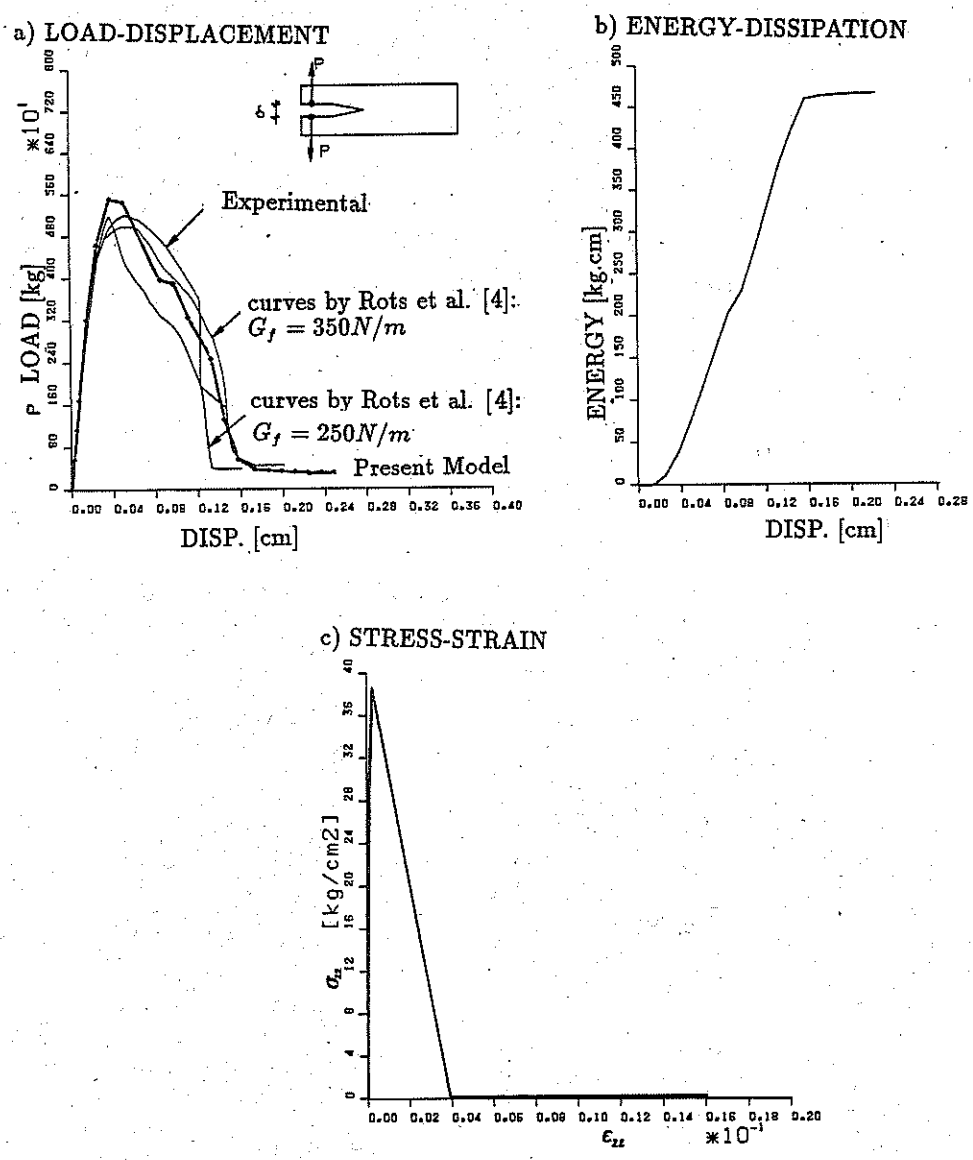
a) LOAD-DISPLACEMENT
P
δ
P
Experimental
curves by Rots et al. [4]:
$G_f = 350N/m$
curves by Rots et al. [4]:
$G_f = 250N/m$
Present Model
P LOAD [kg] *10¹
DISP. [cm]
b) ENERGY-DISSIPATION
ENERGY [kg.cm]
DISP. [cm]
c) STRESS-STRAIN
σ_{zz} [kg/cm2]
ϵ_{zz} *10⁻¹

Fig. 9(a–c)

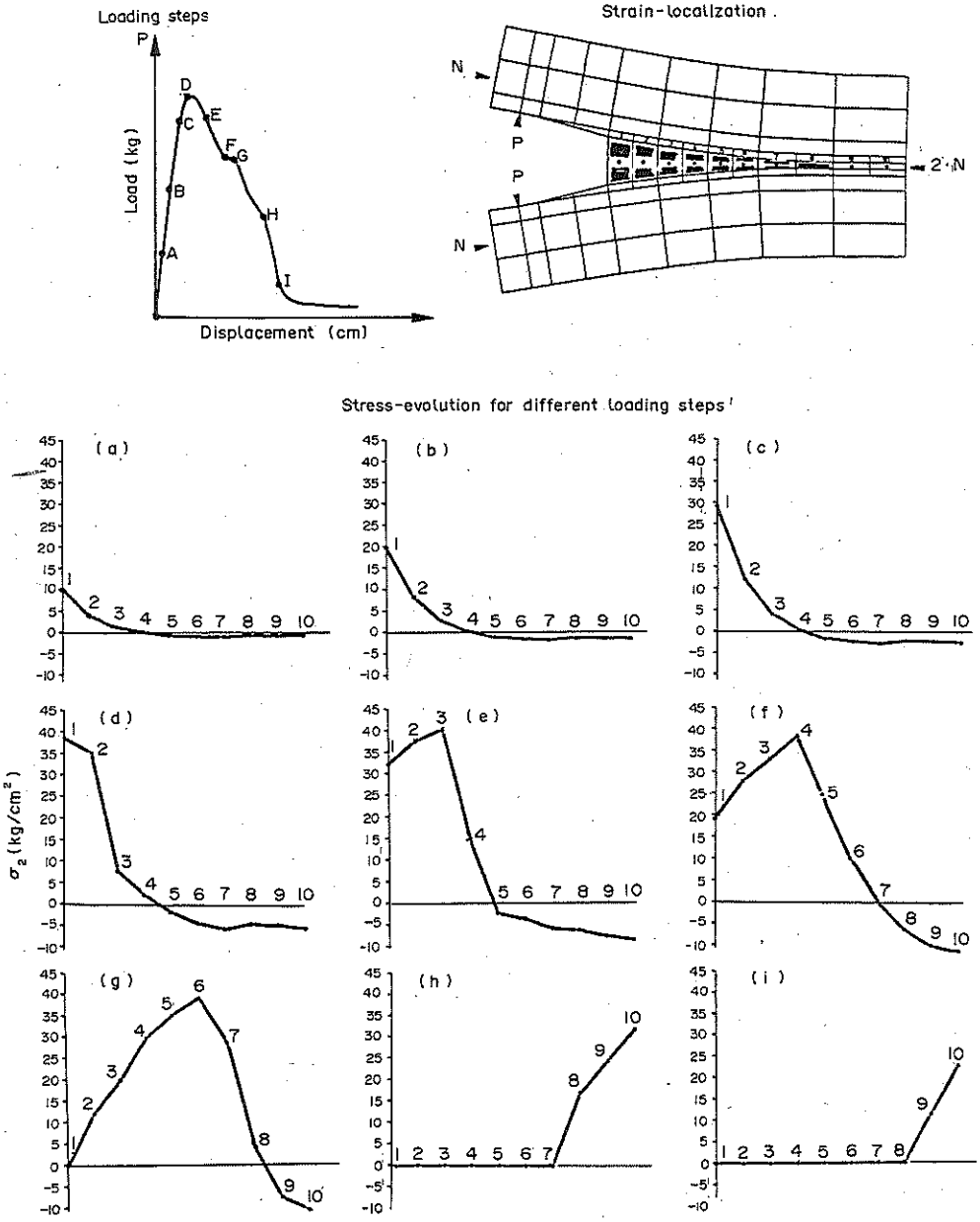

Fig. 9(d)

Fig. 9. *Prestressed beam.* (a) Load–displacement; (b) energy–dissipation; (c) stress–strain in the more damaged integrating point; (d) localization of cracking, and stress evolution.

11. CONCLUSIONS

In this paper a plastic damage model for finite element nonlinear analysis of concrete has been presented. The model allows the accurate reproduction of the nonlinear behaviour of concrete under tension and compression states, including elastic and plastic stiffness degradation effect. The accuracy obtained in the example analysed shows that it can be successfully applied for nonlinear analysis of both plain and reinforced concrete structures.

REFERENCES

[1] Z. Bažant, Mechanics of distributed cracking. *Appl. Mech. Rev.* **39,** 675–705 (1986).
[2] R. De Borst and P. Nauta, Smeared crack analysis of reinforced concrete beams and slabs failing in shear. *Proc. Int. Conf. on Computer-Aided Analysis and Design of Concrete Strucures*, Vol. 1, pp. 261–273. Pineridge Press, Swansea (1984).
[3] Z. Bažant and B. Oh, Crack band theory for fracture of concrete. *Mat. Construct.* (*RILEM*) **16,** 155–177 (1983).
[4] J. G. Rots, P. Nauta, G. Kusters and J. Blaauwendraad, Smeared crack approach and fracture localization in concrete. *Heron* **30,** Delft, Netherlands (1985).
[5] E. Oñate, J. Oliver and G. Bugeda, Finite element analysis of nonlinear response of concrete dams subjected to internal loads, *Europe–US Symposium on Finite Element Methods for Nonlinear Problems* (Edited by Bergan, Bathe and Wunderlich). Springer, Trondheim (1986).
[6] S. Oller, Un modelo de "daño continuo" para materiales friccionales. Tesis Doctoral, Departamento de Estructuras, Universitat Politècnica de Catalunya, Barcelona, España (1988).
[7] J. Lubliner, S. Oller, J. Oliver and E. Oñate, A plastic damage model for nonlinear analysis of concrete. Paper submitted to *Int. J. Solids Struct.* (1988).
[8] L. E. Malvern, Introduction to the Mechanics of a Continuous Medium. Prentice Hall, Englewood Cliffs, N.J. (1969).
[9] J. Prodgorski, General failure criterion for isotropic media. *J. Engng Mech.* **111** (1985).
[10] H. B. Kupfer, H. Hilsdorf and H. Rusch, Behavior of concrete under biaxial stresses. *J. ACI* **66** (1969).
[11] E. Tasuji, F. Slate and A. Nilson, Stress–strain response and fracture of concrete in biaxial loading. *J. ACI* **75,** 306–312 (1978).
[12] E. Oñate, S. Oller, J. Oliver and J. Lubliner, A constitutive model of concrete based on the incremental theory of plasticity. *Engng Comput.* **5,** 4 (1988).
[13] E. Oñate, S. Oller, J. Oliver and J. Lubliner, A fully elastoplastic constitutive model for nonlinear analysis of concrete, *Proc. Second Int. Conf. Advances in Numerical Methods in Engineering, Theory and Application-NUMETA* (Edited by G. Pande and J. Middleton). Martinus Nijhoff, Swansea (1987).
[14] E. Oñate, S. Oller, J. Oliver and J. Lubliner, A constitutive model for cracking of concrete based on the incremental theory of plasticity, in *Proc. Int. Conf. Computational Plasticity* (Edited by D. R. J. Owen, E. Hinton and E. Oñate), Part 2, pp. 1311–1327. Pineridge Press, Barcelona (1987).
[15] S. Oller, J. Oliver, J. Lubliner and E. Oñate, Un modelo constitutivo de daño plástico para materiales friccionales—Part I: Variables fundamentales, funciones de fluencia y potencial. Paper submitted for publication in *Revista Internacional de Metodos Numéricos para el Cálculo y Diseño en Ingeniería* (España) (1968).
[16] J. Oliver, S. Oller and E. Oñate, Modelos elasto–plásticos para simulación numérica de procesos de fractura, in *Methodos Numéricos Applicados a la Mecánica de Fractura* (Edited by J. Oliver, M. Elices, E. Oñate and M. Astiz), pp. 27–60. Centro Internacional de Métodos Numéricos en Ingeniería, Barcelona (1988).
[17] R. De Borst and P. Vermeer, Non-associated plasticity for soils, concrete, and rock. *Heron* **29,** Delft, Netherlands (1984).
[18] S. Oller, J. Oliver, J. Lubliner and E. Oñate, Un modelo constitutive de daño plástico para materiales friccionales—Parte II: Generalización para procesos con degradación de rigidez. Ejemplos—Paper submitted for publication in: "Revista Internacional de Metodos Numéricos para el Cálculo y Diseño en Ingeniería" (España) (1988).
[19] J. C. Simo and J. M. Ju, Strain and stress based continium damage model-Part I: Formulation. *Int. J. Solids Struct.* **23,** 281–841 (1987).
[20] J. Oliver, A consistent characteristic length for smeared cracking models. Paper submitted to *Commun. appl. numer. Method* (1988).
[21] M. Cervera, E. Hinton and O. Hassan, Nonlinear analysis of reinforced plate and shell structures using 20-nodes isoparametric brick elements. *Comput. Struct.* **25,** 845–870 (1987).
[22] K. Willam and J. M. Sobh, Bifurcation analysis of tangencial material operators, In *Int. Conf. on Num. Methods in Engng., Theory and Applications-NUMETA* (Edited by G. Pande and J. Middleton). Martinus Nijhoff, Swansea (1987).

(*Received for publication* 16 *November* 1988)